

A New Approach to Statistics of Cosmological Gamma-Ray Bursts

M. Böttcher^{1,2} & C. D. Dermer²

Submitted to the Astrophysical Journal

ABSTRACT

We use a new method of analysis to determine parameters of cosmological gamma-ray bursts (GRBs), assuming that their distribution follows the star-formation history of the universe. Spectral evolution is calculated from the fireball/blast wave model, and used to evaluate the measured peak flux, duration, and νF_ν peak photon energy for a GRB source occurring at a given redshift and with given values of total energy, baryon-loading and environmental parameters. We then fit model distributions of GRB sources to the observed peak-flux size, duration and νF_ν peak photon energy distributions. Implications for parameters and source models of GRBs are discussed. The ability of the blast wave model to reproduce the three observed GRB distributions self-consistently and simultaneously yields strong support for the external shock model of GRBs, and is in accord with the scenario where GRBs originate from events involving the collapse of massive stars.

Subject headings: cosmology: theory — gamma-rays: bursts — gamma-rays: theory — radiation mechanisms: non-thermal

1. Introduction

The extragalactic origin of GRBs has been confirmed with the discovery of X-ray, optical and radio afterglows of GRBs as a result of the Italian-Dutch Beppo-SAX mission (e.g., Costa et al. 1997; van Paradijs et al. 1997; Frail 1998). At present, there are 4 GRBs with redshifts obtained from emission line measurements of host galaxy counterparts. These are GRB 980425 at redshift $z = 0.0084$ (Kulkarni et al. 1998a), GRB 970508 at $z = 0.835$ (Bloom et al. 1998a), GRB 980703 at $z = 0.966$ (Djorgovski et al. 1998), and GRB 971214 at $z = 3.418$ (Kulkarni et al. 1998b). The redshift inferred for GRB 980425 depends on the validity of the GRB 980425/SN1998bw

¹Rice University, Space Physics and Astronomy Department, MS 108
6100 S. Main Street, Houston, TX 77005 – 1892, USA

²E. O. Hulbert Center for Space Research, Code 7653,
Naval Research Laboratory, Washington, D. C. 20375-5352

association (Galama et al. 1998). The host galaxy redshift of GRB 970508 supports the original redshift report obtained through absorption line measurements in its fading optical counterpart (Metzger et al. 1997), and is strengthened by the recent Beppo-SAX announcement (Piro et al. 1998) of a redshifted iron fluorescence feature found in the spectrum of its fading X-ray counterpart between $\approx 2.5 \times 10^4$ and 6×10^4 s following GRB 970508. ASCA follow-up observations of GRB 970828 localized with BATSE on CGRO also reveal an Fe feature in its spectrum, indicating that this GRB lies at $z = 0.33^{+0.09}_{-0.06}$ (Yoshida 1998). In addition, GRB 970228 is inferred to originate from a source at $1.5 \lesssim z \lesssim 2.6$ due to the lack of strong emission lines in the extremely blue, candidate host galaxy (Fruchter 1998a). The redshift of GRB 980329 is plausibly at $z \cong 5$ due to the R-band dropout observed in the spectrum of its dusty host galaxy (Fruchter 1998b; Reichart et al. 1998).

It is not possible to construct a reliable GRB redshift distribution from the statistics of seven GRBs whose redshifts are obtained through a variety of methods. Except for GRB 980425, however, whose nature remains controversial, the obtained redshifts place most GRBs at the cosmological epoch of active star formation. Several models for the origin of GRBs, such as the collapsar/hypernova scenario (Woosley 1993; Paczyński 1998) or the supranova scenario of Vietri & Stella (1998), suggest that GRBs are physically related to recent star formation. Their cosmological distribution should therefore trace the star formation history of the universe (Totani 1997). An origin of GRBs involving stellar collapse events is also in accord with the small measured offsets of fading transient GRB counterparts with respect to the disks of the candidate host galaxies (Kulkarni 1998). By contrast, a larger offset is expected in the compact object coalescence scenario (e.g., Eichler et al. 1989; Narayan, Paczyński, & Piran 1992) and, moreover, the redshift distribution of GRBs in this scenario is not required to follow the star formation history of the universe due to the large time delays between the formation and merging of compact object binaries.

Wijers et al. (1998) showed that the assumption of a GRB rate proportional to the observed star formation rate (Lilly et al. 1996, Madau et al. 1996), together with a standard-candle assumption on the intrinsic burst luminosity, provides a reasonable description of the observed BATSE/PVO GRB size distribution, whereas Krumholz et al. (1998) demonstrated that a variety of luminosity and redshift distributions of cosmological GRBs are consistent with the observed size distribution. This indicates that the size distribution data alone do not sufficiently constrain GRB parameters, in particular their luminosity and redshift distributions. Recently, Krommers et al. (1998) have included very faint, “non-triggered” BATSE GRBs in a size distribution study and demonstrated that even this improved data set cannot confidently distinguish between a GRB rate tracing the star formation rate and one tracing the redshift distribution of AGNs.

Previous theoretical GRB size distribution studies have either used simple, non-evolving representations of the intrinsic burst spectra, such as a thermal bremsstrahlung spectrum (Fenimore et al. 1993) or a single power-law (Krumholz et al. 1998), or have summed over a sample of observed, time-integrated spectra (Fenimore & Bloom 1995, Wijers et al. 1998, Krommers et al.

1998). Mallozzi et al. (1996) demonstrated that the assumed intrinsic spectral shape of GRBs has a significant influence on the results of theoretical GRB size distribution studies.

The first attempt to combine size distribution studies with other statistical properties was done by Fenimore & Bloom (1995), who deduced a typical distance scale for GRBs from the observed effect of time dilation on the burst duration by comparing the brightest and dimmest BATSE bursts. They found that in order to explain a time dilation by a factor of 2, the dimmest bursts had to be located at $z > 6$. However, they pointed out that the implied isotropic burst luminosity was inconsistent with the observed size distribution, even in the case of a strong cosmological evolution of the comoving burst rate and of the luminosity if both evolutions are parametrized as power-laws in $(1 + z)$. However, the significance of the observed peak flux – duration correlation is highly controversial. Mitrofanov et al. (1993) did not find any evidence for time dilation between dim and bright bursts, while Norris et al. (1994) deduced a maximum redshift of $z \sim 2.25$ for the dimmest bursts from time dilation effects.

Here we demonstrate the importance of considering additional statistical properties to constrain the intrinsic and environmental properties of GRB fireballs. These include the duration distribution and the distribution of peak energies E_p of the time-averaged νF_ν spectra of GRBs. The duration distribution of BATSE GRBs shows a pronounced bimodality (Kouveliotou et al. 1993) between short ($t_{50} \lesssim 0.5$ s) and long ($t_{50} \gtrsim 3$ s) bursts. This has been interpreted as evidence for two physically distinct source populations by Katz & Cane (1996), who found that the $\langle V/V_{max} \rangle$ distribution of the populations of short and long bursts are significantly different from each other. Both populations show evidence for a cosmological origin ($\langle V/V_{max} \rangle < 0.5$), but the long bursts with $\langle V/V_{max} \rangle = 0.282 \pm 0.014$ are located at larger distances and/or exhibit stronger cosmological evolution than the short bursts with $\langle V/V_{max} \rangle = 0.385 \pm 0.019$.

The νF_ν peak energies E_p vary from burst to burst, although most are between ≈ 50 keV and 1 MeV (Mallozzi et al. 1997; Strohmayer et al. 1998). Assuming that the range of E_p intrinsic to the burst sources does not evolve with redshift, Mallozzi et al. (1995) found that the E_p vs. peak flux distribution of BATSE bursts indicates a maximum redshift range of $(1 + z_1)/(1 + z_{100}) = 1.86^{+0.36}_{-0.24}$ between bursts with peak fluxes of 1 and 100 photons $\text{cm}^{-2} \text{ s}^{-1}$, respectively.

Except for the assumptions of a redshift distribution and a phenomenological burst luminosity distribution, previous work has not employed detailed predictions of theoretical blast-wave models for the peak power and temporal evolution of GRB spectra to model the observed statistics of GRBs. In this paper, we use a parametric description of the spectrum and spectral evolution predicted by the external shock model for cosmological GRBs (Dermer et al. 1998a) to calculate self-consistently the peak flux of a GRB at a given redshift, its duration t_{50} , and the observed peak energy E_p of the νF_ν spectrum. Assuming that GRBs trace the star formation history of the universe, this analysis helps to constrain not only the total energy of GRBs, but additional parameters such as the initial Lorentz factor (or baryon loading factor) Γ_0 of the GRB blast wave,

the total energy E_0 deposited into the blast wave, the density of the circumburster material (CBM), and the equipartition factor q , which parametrizes the magnetic field strength and efficiency of electron acceleration in the blast wave.

In Section 2, we present the model equations for a GRB from a fireball/blast wave which is energized, decelerates, and radiates by its interaction with a smooth CBM. We apply BATSE triggering criteria to this model in order to extract measured values of peak flux, duration and peak energy. A function describing the star formation history of the universe is given. In Section 3, we calculate peak-flux size, t_{50} , and E_p distributions for a mono-parametric description of GRBs, and for a GRB model involving ranges of baryon loading factors and total fireball energies. Fits to the observed distributions are presented. Results are discussed in Section 4, and we summarize with implications for source models of GRBs.

2. Peak Fluxes, Peak Energies, and Burst Durations

Following the treatment given by Dermer et al. (1998a), the photon number spectrum from a GRB located at redshift z is parametrized by the expression

$$\Phi(\epsilon, t; z) = \frac{1}{4\pi d_L^2 \epsilon^2 m_e c^2} \frac{(1 + \frac{v}{\delta}) P_p(t)}{[\epsilon/\epsilon_p(t)]^{-v} + (v/\delta) [\epsilon/\epsilon_p(t)]^\delta}, \quad (1)$$

where $\epsilon = E/(m_e c^2)$ is the dimensionless photon energy, d_L is the luminosity distance to the burst, v and δ are the asymptotic low-energy and high-energy νF_ν slopes of the GRB spectrum (throughout this study we use $v = 4/3$ and $\delta = 0.2$), and

$$\epsilon_p(t) = 3.0 \cdot 10^{-8} \frac{q n_0^{1/2} \Gamma_0^4}{1+z} \begin{cases} x^{-\eta/2} & \text{for } 0 \leq x < 1 \\ x^{-4g-\eta/2} & \text{for } 1 \leq x \leq \Gamma_0^{1/g}. \end{cases} \quad (2)$$

Here, $q = \sqrt{\xi_H(r/4)} \xi_e^2$ is the combined equipartition factor, containing the magnetic field equipartition factor ξ_H , the electron equipartition factor ξ_e , and the shock compression ratio r , and Γ_0 is the initial bulk Lorentz factor or baryon loading factor of the blast wave. The term η is the power-law index of the surrounding CBM density structure, given by the smoothly varying function

$$n(x) = n_0 x^{-\eta}, \quad (3)$$

which is assumed to be isotropically distributed about the source of the GRB. For simplicity, we let $\eta = 0$ in the calculations presented here.

The term $x = R/R_d$ is the radial coordinate R in units of the deceleration radius R_d , and is related to the observing time t by

$$x = \begin{cases} \frac{t}{t_d} & \text{for } 0 \leq x \leq 1 \\ \left[(2g+1) \frac{t}{t_d} - 2g \right]^{1/(2g+1)} & \text{for } 1 \leq x \leq \Gamma_0^{1/g}. \end{cases} \quad (4)$$

Here t_d is the deceleration time scale of the blast wave, given by

$$t_d = \frac{1+z}{c \Gamma_0^{8/3}} \left[\frac{(3-\eta) E_0}{4\pi n_0 m_p c^2} \right]^{1/3}, \quad (5)$$

and g parametrizes the radiative regime. For a non-radiative (adiabatic) blast wave, $g = 3/2 - \eta$, while $g = 3 - \eta$ describes a fully radiative blast wave. Throughout this study, we assume that the blast wave is uncollimated. Beaming can be approximately implemented in the prompt and early afterglow phases of a GRB by replacing the total energy E_0 with the quantity $4\pi(\partial E_0/\partial\Omega)$, where $\partial E_0/\partial\Omega$ is the energy radiated per steradian into the solid angle element whose normal is directed within an angle $\lesssim 1/\Gamma_0$ of the direction to the observer. The peak νL_ν luminosity $P_p(t)$ depends on the parameters of the model according to the relation

$$P_p(t) = \frac{c(2g-3+\eta)(4\pi m_p c^2)^{1/3}}{2g(v^{-1} + \delta^{-1})(1+z)^2} n_0^{1/3} E_0^{2/3} \Gamma_0^{8/3} \begin{cases} x^{2-\eta} & \text{for } 0 \leq x < 1 \\ x^{2-\eta-4g} & \text{for } 1 \leq x \leq \Gamma_0^{1/g}. \end{cases} \quad (6)$$

Using Eq. (1), we determine the peak flux $\Phi_p(z)$ of a GRB, averaged over the BATSE trigger time scale Δt in the 50 - 300 keV energy range, by scanning through t_1 and finding the maximum of the expression

$$\Phi_p(z) = \max_{t_1} \left\{ \frac{1}{\Delta t} \int_{t_1}^{t_1 + \Delta t} dt \int_{\epsilon_1}^{\epsilon_2} d\epsilon \Phi(\epsilon, t; z) \right\}, \quad (7)$$

where $\epsilon_1 = 50/511$ and $\epsilon_2 = 300/511$. A burst triggers BATSE if $\Phi_p(z) > \Phi_{\text{trig}}$, where Φ_{trig} is the trigger threshold, which depends on the trigger time scale. For $\Delta t = 1024$ ms, $\Phi_{\text{trig}} \approx 0.2$ photons $\text{cm}^{-2} \text{s}^{-1}$, while for $\Delta t = 64$ ms, $\Phi_{\text{trig}} \approx 1$ photon $\text{cm}^{-2} \text{s}^{-1}$ (Fishman et al. 1994). The trigger criterion corresponding to $\Delta t = 1024$ ms involves a selection bias toward bursts with durations $\gtrsim 1$ s. Shorter bursts with the same peak flux are less likely to trigger the GRB telescope because the total number of detected photons during the trigger time scale is smaller. This effect is reflected in the larger trigger threshold for bursts which trigger on the 64 ms time scale than those which trigger on the 1024 ms time scale.

For a given peak flux value Φ_p and a given set of GRB parameters, we find a limiting redshift $z_{\text{max}}(\Phi_p)$ at which the GRB produces a peak flux $\Phi_p(z_{\text{max}}) = \Phi_{\text{trig}}$. Fig. 1 illustrates how z_{max} of a standard GRB varies with Γ_0 and q . For a given value of q , the peak flux increases with increasing Γ_0 until E_p attains values greater than the photon energies of the detector triggering range. At larger values of Γ_0 , the emission recorded by a detector is dominated by the synchrotron emissivity spectrum $F_\nu \propto \nu^{1/3}$ produced by a distribution of electrons with a low-energy cutoff. Because this portion of the spectrum is so hard, the peak flux, and therefore z_{max} , declines at larger values of Γ_0 , as shown in Fig. 1. The Lorentz factor $\bar{\Gamma}_0$ of a fireball which produces the maximum peak flux in a detector sensitive to photons with energy E_d is given by $\bar{\Gamma}_0 \approx 75 [(1+z)E_d/(m_e c^2 q n_0^{1/2})]^{1/4}$, using eq. (2). The nominal BATSE triggering range, as noted above, is $50 \text{ keV} \leq E_d \leq 300 \text{ keV}$.

A cumulative size distribution in a matter-dominated Friedmann cosmology is then calculated from the relation

$$\dot{N}(> \Phi_p) = \frac{c}{H_0} \int_0^{z_{\max}(\Phi_p)} dz \frac{\dot{n}_{GRB}(z) d_L^2}{(1+z)^4 \sqrt{1+2q_0 z}}, \quad (8)$$

(see, e.g., Dermer 1992) with

$$d_L = \frac{c}{H_0 q_0^2} \left[z q_0 + (q_0 - 1) (\sqrt{2q_0 z + 1} - 1) \right], \quad (9)$$

where $\dot{n}_{GRB}(z)$ is the comoving burst rate per comoving unit volume. The differential size distribution $\dot{N}(\Phi_p)$ is evaluated by numerically differentiating the cumulative size distribution with respect to Φ_p . We use $H_0 = 65 \text{ km s}^{-1} \text{ Mpc}^{-1}$, $q_0 = 0.5$, $\Omega = 1$, and $\Lambda = 0$, unless otherwise stated.

We assume that $\dot{n}_{GRB}(z)$ is proportional to the star formation rate (SFR), for which we use a simple representation of the function shown in Madau et al. (1998):

$$SFR(z)[M_\odot \text{ yr}^{-1} \text{ Mpc}^{-3}] = \begin{cases} 10^{-3} \cdot 10^{z+1} & \text{for } z \leq 1.1 \\ 0.13 & \text{for } 1.1 < z \leq 2.8 \\ 4.2 \cdot 10^{-0.4(z+1)} & \text{for } z > 2.8. \end{cases} \quad (10)$$

The νF_ν peak energy of the burst spectrum as a function of redshift is evaluated at the time $t = t_d$ of peak power output of the GRB using eq. (2). Thus $E_p/(m_e c^2) = 3.0 \times 10^{-8} q n_0^{1/2} \Gamma_0^4 / (1+z)$. For the duration distribution, we calculate t_{50} as the duration between the times when 25% and 75% of the total photon fluence in the 50 – 300 keV band (from eq. [1]) has been received. In Fig. 2 we plot t_{50} as a function of Γ_0 and q for a standard GRB located at $z = 1$. For small values of Γ_0 , for which E_p is below or within the detector energy range, t_{50} is proportional to the deceleration time t_d . For larger Γ_0 , E_p is above the detector energy range, and the burst duration is determined by the time it takes for the νF_ν peak of the evolving burst spectrum to sweep through the detector energy range. For the parameters given here, t_{50} is only weakly dependent on the initial bulk Lorentz factor in the high- Γ_0 limit. Using the asymptotic forms of eq. (1) and realizing that most photons are produced after $E_p(t)$ has swept through the detector energy range, one can analytically show that $t_{50} \propto t_d \Gamma_0^{(2g+1)/(g+\eta/8)} \propto \Gamma_0^{(1/g)-(2/3)}$ if $\Gamma_0 \gg \bar{\Gamma}_0$, where the last expression holds when $\eta = 0$. As is evident from Fig. 2, the burst duration t_{50} is positively correlated with the equipartition parameter q .

To compute the E_p and t_{50} distributions, we first calculate a redshift distribution

$$\dot{N}(z) = \dot{N}(\Phi_p) \left| \frac{d\Phi_p}{dz} \right| \quad (11)$$

and then evaluate

$$\dot{N}(t_{50}) = \dot{N}(z) \left| \frac{dz}{dt_{50}} \right| \quad (12)$$

and analogously for E_p . The derivatives in eqs. (11) and (12) are calculated numerically.

We caution that our analysis does not take into account any effects due to the instrumental noise or the diffuse radiation backgrounds recorded by the BATSE detectors. The actual t_{50} and t_{90} durations of a GRB are expected to be somewhat longer than measured because the additional background noise will dominate the emissions from a GRB at early and late times, particularly for weak GRBs. The actual E_p distribution of those GRBs which trigger BATSE is, however, not expected to be much different from the measured E_p distribution, because the background spectrum is subtracted in the spectral analyses which yield E_p (see, e.g., Mallozzi et al. 1995).

3. Comparison with Observed Distributions

We first applied the formalism described in the previous section to calculate size, E_p , and duration distributions from cosmological GRBs with a single set of values for the burst parameters. The theoretical distributions were compared with the size and duration distributions from the Third BATSE GRB catalog as compiled by Meegan et al. (1996), and to the E_p distribution of Mallozzi et al. (1997). The values of E_p were evaluated by Mallozzi et al. (1997) by fitting the GRB spectrum from the 4B catalog (Meegan et al. 1997) with the Band function (Band et al. 1993). In the first step of our analysis we use the trigger time scale $\Delta t = 1024$ s, corresponding to a peak flux threshold of $\Phi_{trig} = 0.2$ photons $\text{cm}^{-2} \text{s}^{-1}$. This is the trigger criterion used to extract the size distribution data shown in Meegan et al. (1996) and in our Figs. 3, 6, and 7. We note that our analysis is properly applied to data sets which are produced by uniform triggering criteria, but that the E_p distribution might be biased with respect to the duration and size distributions since the E_p data can be obtained only for the brighter GRBs. Moreover, the E_p analysis uses 16 energy channel data, whereas the peak fluxes are based on the four energy channel discriminator data (R. Mallozzi, private communication, 1998). A uniform selection criterion for the size, duration and E_p distributions should be considered in future studies.

The best match of our theoretical size distribution with the data which was simultaneously consistent with the peaks in the E_p and the t_{50} distributions was achieved for $E_0 = 8 \cdot 10^{52}$ erg, $\Gamma_0 = 130$, $n_0 = 10^5 \text{ cm}^{-3}$, $g = 1.8$, and $q = 2.5 \cdot 10^{-4}$. The value $q = 2.5 \cdot 10^{-4}$ is based on the results of Chiang & Dermer (1998), who argue that such a small equipartition parameter is required in order to prevent rapid synchrotron cooling. A larger value of q would result in a low-energy synchrotron spectrum $\Phi(\epsilon) \propto \epsilon^{-3/2}$, inconsistent with the observed hard low-energy asymptotes of BATSE GRB spectra (Band et al. 1993, Crider et al. 1997, Preece et al. 1998). Figs. 3 – 5 show the size, E_p , and t_{50} distributions, respectively, from this mono-parametric burst population. The model results for the size distributions are not completely smooth due to numerical scatter and because they are only evaluated at the peak flux values where there are data.

The fit to the size distribution results in an acceptable reduced $\chi^2_\nu = 0.51$ (7 degrees of freedom). Our model distribution yields $\langle V/V_{max} \rangle = 0.268$, which agrees well with the result of Katz & Canel (1996) for the population of long bursts quoted in Section 1. The size distribution

data used to make the model comparison includes only GRBs which trigger on the 1024 ms time scale. Thus, although the long GRBs account for only 75% of the total, they constitute a significantly larger fraction of the bursts exceeding the 1024 ms trigger criterion. A direct comparison with the results of Katz & Canel (1996) is therefore valid. The normalization of our model size distribution requires $\dot{n}_{\text{GRB}}(z) = 1.63 \cdot 10^{-7} SFR/M_{\odot}$, which yields a local GRB rate $\dot{n}_{\text{GRB}}(z = 0) = 1.63 \text{ GRBs yr}^{-1} \text{ Gpc}^{-3}$. Assuming a local galaxy number density of $4.8 \cdot 10^{-3} \text{ Mpc}^{-3}$ (Wijers et al. 1998), this is equivalent to a local GRB rate of 0.34 GEM (Galactic events per Myr), or 1 event in 2.9 Myr per galaxy. This rate is a factor of 14 higher than the result of Wijers et al. (1998).

We point out that this fit is not unique. There is at least one ambiguity in the sense that equally good fits can be achieved by assuming a lower CBM density n_0 and a higher initial bulk Lorentz factor Γ_0 , keeping the product $\sqrt{n_0} \Gamma_0^4$ constant (for example, $n_0 = 100 \text{ cm}^{-3}$ and $\Gamma_0 \approx 300$ yields just as good a fit as the parameters quoted above). The reason for this ambiguity lies in the fact that the peak flux, E_p , and t_d all depend only on the product $n_0 \Gamma_0^8$ (see eqs. [6], [2], and [5]). An average density of $n_0 \sim 10^2 - 10^5 \text{ cm}^{-3}$ seems to be appropriate if GRBs are correlated with star-forming regions. Our results are very sensitive to the value of g which parametrizes the radiative regime and thus determines the luminosity of the GRB. This is illustrated in Fig. 3, where we also plot the size distributions resulting from more radiative blastwaves with $g = 2$ and almost non-radiative blastwaves with $g = 1.6$ for comparison. Our results are also rather sensitive to the cosmological parameters. In Fig. 6, we show the resulting size distributions of our mono-parametric burst population for different values of q_0 and H_0 .

As is evident from eq. (2) and from Figs. 1 and 2, all three distributions are fairly sensitive to the equipartition parameter q . Assuming that the value of E_0 is fixed at $\sim 10^{53} \text{ erg}$, thought to be typical of cosmological GRBs (Waxman 1997; Bloom et al. 1998b; Kulkarni et al. 1998b), the value of q is constrained to the value adopted in our fit. The faintest detectable bursts resulting from this mono-parametric model are located at a redshift of $z_{\text{max}} = 1.75$. This is consistent with the measured redshifts of GRB 970508 (Metzger et al. 1997) and GRB 980703 (Djorgovski et al. 1998), but is incompatible with the redshift of 3.42 measured for the proposed host galaxy of GRB 971214 (Kulkarni et al. 1998b).

Although the size distribution is modelled well and the expected mean values of t_{50} and E_p are in the range measured for these burst properties, the theoretical duration and E_p distributions are too narrow to explain the spread in these observables purely by time dilation and cosmological redshift effects (which are explicitly taken into account in the model parametrization). Moreover, the bimodality of the burst duration cannot be explained with a mono-parametric burst model. A more realistic approach is thus to consider a limited range in the allowed values of several parameters. In the following, we consider a range of baryon loading factors and total fireball energies.

Dermer et al. (1998a, 1998b) argue that there could be a wide distribution in the baryon

loading factor of GRB fireballs, of which only those sources with νF_ν peaks between ~ 50 keV – several MeV have been detected due to the triggering criteria of currently operating GRB monitors and the limitations of telescopes at X-ray and \gg MeV energies. Detectability of burst sources with smaller values of Γ_0 , corresponding to values of $\Gamma_0 \ll 130$ when $n_0 = 10^5 \text{ cm}^{-3}$ in our example, is strongly reduced because most of the flux will be emitted at energies below the sensitivity threshold of BATSE. The same is true, though to a lesser extent, for fireballs which produce blast waves with $\Gamma_0 \gg 130$, again for the case when $n_0 = 10^5 \text{ cm}^{-3}$. Thus we expect that the size distribution observed from a population of burst sources with a variety of Γ_0 values will not deviate significantly from our mono-parametric population considered above. However, due to the strong dependence of the peak energy E_p on Γ_0 through eq. (2), we expect that the width of the observed E_p distribution may well be a consequence of a range of Γ_0 values with n_0 fixed (so that there is a range of values of the product $n_0 \Gamma_0^8$). The dependence of the burst duration on Γ_0 is weaker, but still considerable. In terms of the deceleration time t_d , we have $t_d \propto \Gamma_0^{-8/3}$, so that a range in Γ_0 will also lead to a broadening of the t_{50} distribution for a fixed value of n_0 .

Furthermore, from estimates of the energetics of GRB 970508 (e.g., Waxman 1997), GRB 980703 (Bloom et al. 1998b), and GRB 971214 (Kulkarni et al. 1998b), not to mention GRB 980425 (Kulkarni et al. 1998a), we know that the total available energy E_0 in the blast wave may well vary from source to source by more than 1 – 2 orders of magnitude. Thus we also assume a range in E_0 .

In order not to introduce too many new parameters, we restrict our analysis to single power-laws in the parameters Γ_0 and E_0 . We therefore let $dN/dy \propto y^{-\alpha}$, where y represents either Γ_0 or E_0 , and α is the index of the distribution. A reasonable match with the observed E_p distribution, which even improves the fit for the size distribution, is found for power-laws with $\alpha = 1$ extending over the ranges $115 \leq \Gamma_0 \leq 160$ and $5 \cdot 10^{52} \text{ erg} \leq E_0 \leq 1.2 \cdot 10^{53} \text{ erg}$. The resulting E_p and t_{50} distributions are shown by the dot-dashed histograms in Figs. 4 and 5, respectively; the size distribution is shown in Fig. 7. As can be seen from Fig. 5, the predicted duration distribution is still significantly narrower than the observed one. We did not find a continuous range in Γ_0 and E_0 which accurately matched the width of the t_{50} distribution. However, this is not surprising because the external synchrotron shock model parametrized by eq. (1) only accounts for the simpler, so-called “Fast-Rise, Exponential Decay” FRED-like burst light curves (see Fishman & Meegan 1995; Dermer et al. 1998b). While the overall spectral shape and luminosity (which determines the size and E_p distribution) may be similar for more complicated, spiky light curves — which could arise from the interaction of the blast wave with an inhomogeneous medium (Dermer & Mitman 1998) — the observed durations might be altered significantly by this effect.

The bimodality of the duration distribution is not reasonably explained by a variety of light curves, and probably indicates a bimodality in parameter space (Katz & Canel 1996). For example, the class of short bursts could be produced by an additional population of less energetic burst sources with smaller baryon contamination (larger Γ_0). The smaller baryon loading might

lead to a more rapid deceleration of the blast wave. Assuming $E_0 = 2.6 \cdot 10^{51}$ erg, $\Gamma_0 = 300$, $g = 2.9$, and $q = 2 \cdot 10^{-5}$, such an additional population would produce bursts with typical duration $t_{50} \sim 0.1 - 0.2$ s and νF_ν peak energies of $E_p \sim 500$ keV and would be detectable out to $z_{max} \sim 0.7$. Our model population of short bursts yields $\langle V/V_{max} \rangle = 0.388$, in agreement with the result of Katz & Canel (1996). Such a short GRB population is also consistent with the observed trend that the shorter bursts are generally harder (higher E_p) than the longer bursts. The dashed curve in Fig. 7 shows the size distribution from this sub-population of short – hard bursts. The lower equipartition parameter required for this fit is plausible because a larger fraction of the swept-up energy is transformed into energy of the magnetic field, implying a higher value of the magnetic-field equipartition factor, ξ_H . If the mechanism responsible for electron acceleration is only weakly dependent on the magnetic-field strength, the balance of acceleration to synchrotron losses of the electrons results in a lower electron equipartition parameter, $\xi_e \propto \xi_H^{-1/2}$, which yields $q \propto \xi_H^{1/2} \xi_e^2 \propto \xi_H^{-1/2}$, indicating that in the case of a higher magnetic field (and a more radiative regime of the blast-wave evolution) the equipartition parameter is expected to be lower. However, this statement is not true if the electrons are accelerated by the 2nd order Fermi process which is strongly dependent on the magnetic-field strength.

We again point out that our choice of parameters for the short – hard population is not unique due to the ambiguity in the parameter $\Gamma_0 n_0^{1/8}$. Independent of the special choice of parameters, however, is the prediction drawn from the blast wave model that the shorter bursts should tend to be harder, which is a consequence of the strong dependence of $t_d \propto \Gamma_0^{-8/3}$ and $E_p \propto \Gamma_0^4$ on the baryon loading factor and the fact that the burst duration is only weakly dependent on the other parameters of the model.

4. Summary and Conclusions

We have used the cosmological blast wave model to fit simultaneously the size, E_p , and t_{50} distribution as observed by BATSE, using an analytical representation of the spectral evolution predicted by the external shock model. The GRB source distribution is assumed to trace the star formation history of the universe. For our standard cosmology ($q_0 = 0.5$, $H_0 = 65$ km s⁻¹ Mpc⁻¹, $\Lambda = 0$), the size distribution, the E_p distribution, and the population of GRBs with durations $t_{50} \gtrsim 0.5$ s can be modeled with a source population characterized by $115 \leq \Gamma_0 \leq 160$, $5 \cdot 10^{52}$ erg $\leq E_0 \leq 1.2 \cdot 10^{53}$ erg, $g = 1.8$, and $q = 2.5 \cdot 10^{-4}$, if the density of the circumburster material is assumed as $n_0 = 10^5$ cm⁻³. Equally good fits can be found for different values of the CBM density, if the product $\sqrt{n_0} \Gamma_0^4$ is held constant. Our results are fairly sensitive to the assumed cosmological parameters and the radiative regime of the blast wave. Our model fit implies a local GRB rate of 1.6 GRBs yr⁻¹ Gpc⁻³ or 0.34 GEM.

The bimodality of the t_{50} distribution can be explained in the context of the present model if a bimodality in GRB source parameter space is assumed. We suggest the existence of a separate

population of short – hard bursts, characterized by a less energetic burst source ($E_0 = 2.6 \cdot 10^{51}$ erg) with smaller baryon contamination ($\Gamma_0 = 300$ when $n_0 = 10^5$ cm $^{-3}$) and blast waves evolving in the highly radiative regime ($g = 2.9$).

The simplified analytic form used to represent the observed spectra from cosmological blast waves provides a reasonable representation of all three statistical distributions considered in this paper, thus lending strong support in favor of the external shock model of GRBs. The width of the observed E_p distribution may be regarded as evidence for the existence of burst sources with a range of baryon loading factors Γ_0 , as suggested by Dermer et al. (1998a). In Dermer et al. (1998b), we discussed the possibility that even burst sources with baryon loading factors outside the range quoted above. Our analysis only weakly constrains the existence of a population of dirty fireballs with lower values of Γ_0 , because these dirty fireballs are largely undetectable for BATSE due to the rapid decline of the observed peak flux in the BATSE photon energy range with decreasing Γ_0 . BATSE is therefore insensitive to a dirty fireball population except for the few events that occur at redshifts $z \ll 1$. The small number of GRBs with $E_p \lesssim 100$ keV in the data shown in Fig. 4 might actually be an artifact of the selection bias mentioned at the beginning of the previous section, namely that E_p can only be determined for bright bursts, while dirty fireballs, producing spectra with low E_p , are intrinsically dim. An additional difficulty in constraining the dirty fireball population is the uncertainty of determining the high-energy spectral index δ of the average GRB spectrum. A higher value of δ than the one used in our model calculations would render the dirty fireballs even harder to detect for BATSE.

By contrast, we find from the present study that a significant number of clean fireball burst sources with Γ_0 much larger than the upper limit quoted above ($\Gamma_0^{\max} n_0^{1/8} \approx 675$ cm $^{-3/8}$) should have been detected by BATSE unless q is strongly dependent on Γ_0 . If q is constant from burst to burst, then extension of the assumed power-law distribution in Γ_0 to higher values would lead to an E_p distribution which is inconsistent with the data unless $dN/d\Gamma_0 \propto \Gamma^{-\alpha_{\max}}$, where $\alpha_{\max} \gtrsim 4$.

We therefore conclude that our analysis is in accord with the existence of a class of dirty fireballs with $E_p \ll 100$ keV which have generally not been detected with BATSE. The existence of a significant fraction of cleaner fireballs than detected by BATSE seems less likely unless q becomes much smaller in the cleaner fireballs. Insofar as clean fireballs with very small values of q could represent the short, hard population of GRBs, this indicates that GRBs have values of the equipartition parameter q which obtain very small values when Γ_0 becomes large.

Our results indicate that most of the faintest bursts detected by BATSE are located at $z \sim 2$. This value remains generally unchanged for different sets of parameters which yield similarly good fits to the observed statistical distributions. This result agrees well with the redshifts determined for several GRBs, but is inconsistent with the redshift $z = 0.0084$ for the host galaxy of SN 1998bw claimed to be associated with GRB 980425, with $z = 3.42$ measured for the candidate host galaxy of GRB 971214, and with the inferred redshift of $z \cong 5$ for GRB 980329 (see Section 1). Given that a range of energies and baryon-loading factors are required to provide adequate fits to the

model distributions, a small number of very weak or very energetic fireballs could account for the low- and high-redshift sources.

In summary, we use a parametrization of the blast wave model to calculate the peak flux, duration, and νF_ν peak energy of a GRB with a prescribed set of intrinsic and environmental parameters. We assume that the evolution of the GRB rate with redshift is proportional to the star-formation history of the universe. By taking into account triggering properties of GRB detectors in our calculations, we make detailed comparison of model distributions with BATSE results for the size, t_{50} , and E_p distributions. For the first time, we have shown how these distributions can be self-consistently modeled and used to extract allowed ranges of fireball energies and baryon-loading factors. Our analysis is in accord with the scenario that GRBs are associated with sites of active star formation. Future work must consider evolutionary behaviors to test compact object coalescence scenarios. We argue that the short, hard GRBs represent a population of cleaner fireballs with small values of the equipartition parameter.

We thank J. Chiang for useful comments. This work is partially supported by NASA grant NAG 5-4055. CD acknowledges support from the Office of Naval Research.

REFERENCES

Band, D., Matteson, J., Ford, L., et al., 1993, *ApJ*, 413, 281

Bloom, J. S., Djorgovski, S. G., Kulkarni, S. R., & Frail, D. A. 1998a, *ApJ*, 507, L105

Bloom, J. S., et al. 1998b, *ApJ*, 508, L21

Chiang, J., & Dermer, C. D., 1998, *ApJ*, in press (astro-ph/9803339)

Costa, E., et al. 1997, *Nature*, 387, 783

Crider, A. W., Liang, E. P., Smith, I. A., et al., 1997, *ApJ*, 479, L39

Dermer, C. D., 1992, *PRL*, Vol. 68, No. 12, 1799

Dermer, C. D., Chiang, J., & Böttcher, M., 1998a, *ApJ*, 513, in press (astro-ph/9804174)

Dermer, C. D., Böttcher, M., & Chiang, J., 1998b, *ApJL*, submitted

Dermer, C. D., & Mitman, K. E., 1998, *ApJ*, submitted (astro-ph/9809411)

Djorgovski, S. G., Kulkarni, S. R., Bloom, J. S., Goodrich, R., Frail, D. A., Piro, L., & Palazzi, E. 1998, *ApJ*, 508, L17

Eichler, D., Livio, M., Piran, T., & Schramm, D. N. 1989, *Nature*, 340, 126

Fenimore, E. E., Epstein, R. I., Ho, C., et al., 1993, *Nature*, 366, 40

Fenimore, E. E., & Bloom, J. S., 1995, *ApJ*, 453, 25

Fishman, G. J., & Meegan, C. A., 1995, *ARAA*, 33, 415

Fishman, G. J., et al. 1994, *ApJS*, 92, 229

Frail, D. 1998, in the Fourth Huntsville Gamma-Ray Burst Symposium, ed. C. A. Meegan, R. D. Preece, & T. M. Koshut (AIP: New York), 563

Fruchter, A. S. 1998a, presentation at “Gamma-Ray Bursts in the Afterglow Era,” 3-6 November, 1998, Rome, Italy

Fruchter, A. S. 1998b, *ApJ*, in press (astro-ph/9810224)

Galama, T. J., et al. 1998, *Nature*, 395, 670

Katz, J. I., & Cane, L. M., 1996, *ApJ*, 471, 915

Kommers, J. M., Lewin, W. H. G., Kouveliotou, C., et al., 1998, *ApJ*, submitted (astro-ph/9809300)

Kouveliotou, C., et al., 1993, *ApJ*, 413, L101

Krumholz, M., Thorsett, S. E., & Harrison, F. A., 1998, *ApJ*, 506, L81

Kulkarni, S., presentation at “Gamma-Ray Bursts in the Afterglow Era,” 3-6 November, 1998, Rome, Italy

Kulkarni, S., et al., 1998a, *Nature*, 395, 663

Kulkarni, S., et al., 1998b, *Nature*, 393, 35

Lilly, S. J., LeFèvre, O., Hammer, F., & Crampton, D., 1996, *ApJ*, 460, L1

Madau, P., Ferguson, H. C., Dickinson, M. E., et al., 1996, *MNRAS*, 283, 1388

Madau, P., Pozzetti, L., & Dickinson, M., 1998, *ApJ*, 498, 106

Mallozzi, R. S., Paciesas, W. S., Pendleton, G. N., et al., 1995, *ApJ*, 454, 597

Mallozzi, R. S., Pendleton, G. N., & Paciesas, W. S., 1996, *ApJ*, 471, 636

Mallozzi, R. S., Pendleton, G. N., Paciesas, W. S., et al., 1997, in 4th Huntsville Symposium on Gamma-Ray Bursts, eds. Meegan, C. A., Preece, R. D., & Koshut, T. M., p. 273

Meegan, C. A., Pendleton, G. N., Briggs, M. S., et al., 1996, *ApJS*, 106, 65

Meegan, C. A., Paciesas, W. S., Pendleton, G. N., et al., 1997, in 4th Huntsville Symposium on Gamma-Ray Bursts, eds. Meegan, C. A., Preece, R. D., & Koshut, T. M., p. 3

Metzger, M. R., Djorgovski, S. G., Kulkarni, S. R., et al., 1998, *Nature*, 387, 878

Mitrofanov, I. G., et al., 1993, in 2nd Compton Symposium, ed. M. Friedlander, N. Gehrels, & D. J. Macomb (New York: AIP Conf. Proc. 280), 761

Narayan, R., Paczyński, B., & Piran, T. 1992, *ApJ*, 395, L83

Norris, J. P., Nemiroff, R. J., Scargle, J. D., et al., 1994, *ApJ*, 424, 540

Paczyński, B., 1998, *ApJ*, 494, L45

Piro, L., et al., 1998, *ApJL*, submitted

Preece, R. D., Briggs, M. S., Mallozzi, R. S., et al., 1998, *ApJ*, 506, L23

Reichart, D. E., et al. 1998, *ApJ*, submitted (astro-ph/9810487)

Strohmayer, T. E., Fenimore, E. E., Murakami, T., & Yoshida, A. 1998, *ApJ*, 500, 873

Totani, T., 1997, *ApJ*, 486, L71

van Paradijs, J., et al. 1997, *Nature*, 386, 686

Vietri, M., & Stella, L., 1998, *ApJ*, 507, L45

Waxman, E. 1997, *ApJ*, 489, L33

Wijers, R. A. M. J., et al., 1998, *MNRAS*, 294, L13

Woosley, S. E. 1993, *ApJ*, 405, 273

Yoshida, A. et al. 1998, presentation at “Gamma-Ray Bursts in the Afterglow Era,” 3-6 November, 1998, Rome, Italy

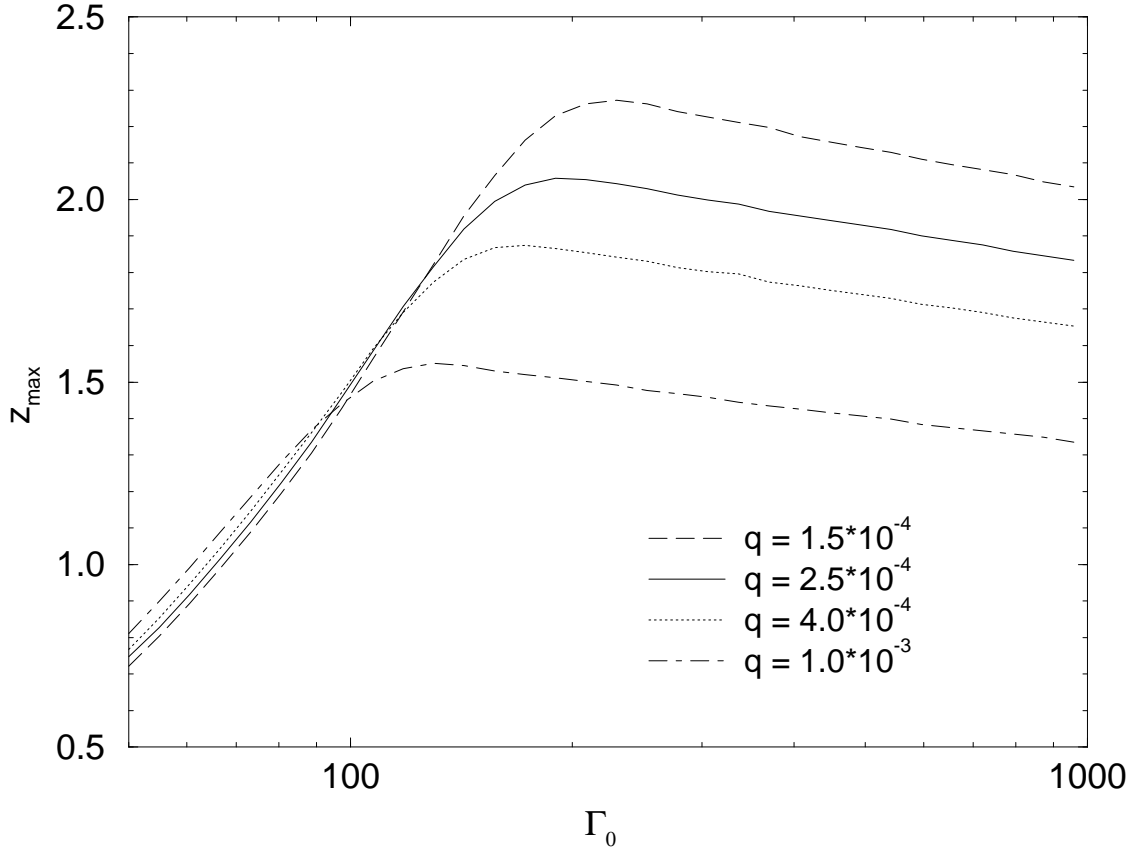


Fig. 1.— The maximum redshift out to which a GRB can be detected above the 1024 ms trigger threshold $\Phi_{lim} = 0.2$ photons $\text{cm}^{-2} \text{ s}^{-1}$, as a function of baryon loading factor Γ_0 and equipartition factor q . Parameters: $E_0 = 10^{53}$ erg, $n_0 = 10^5 \text{ cm}^{-3}$, $g = 1.8$.

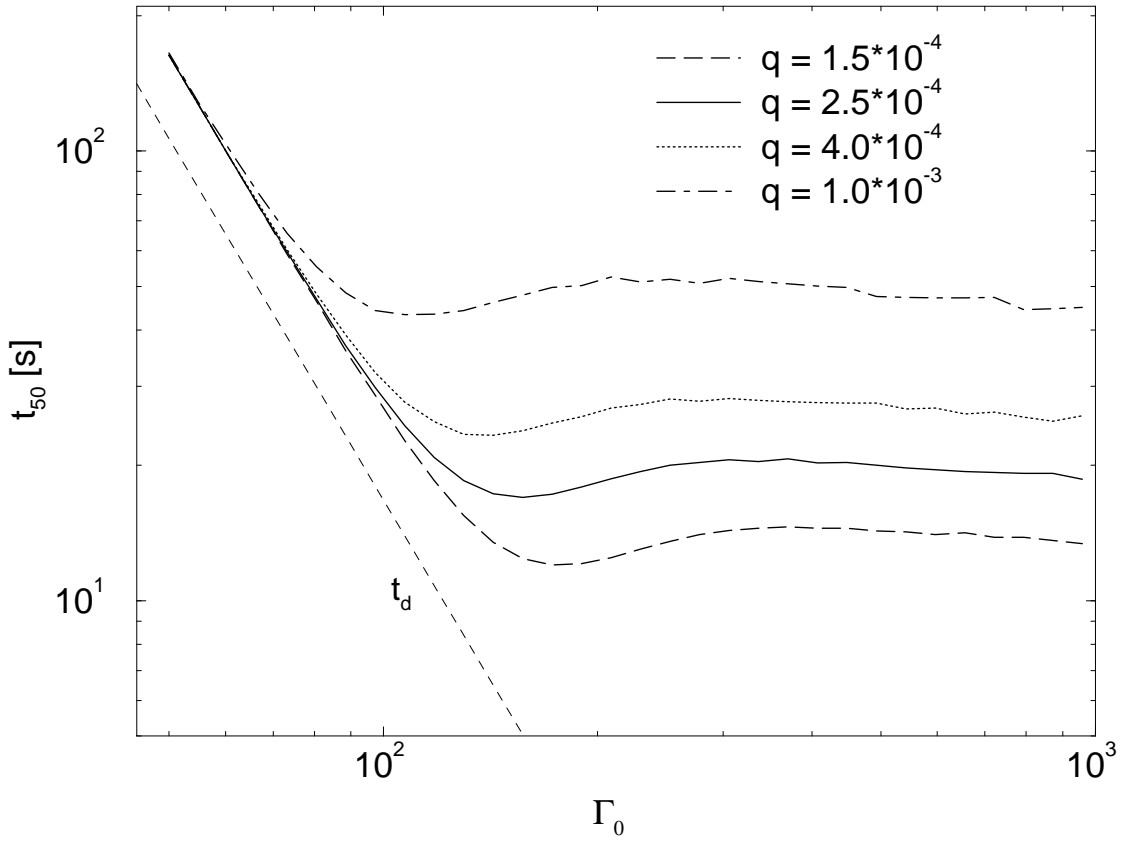


Fig. 2.— Burst duration t_{50} for a standard GRB located at $z = 1$, as a function of Γ_0 and q . Other parameters: $E_0 = 10^{53}$ erg, $n_0 = 10^5$ cm $^{-3}$, $g = 1.8$. The dashed curve shows the deceleration time t_d for comparison.

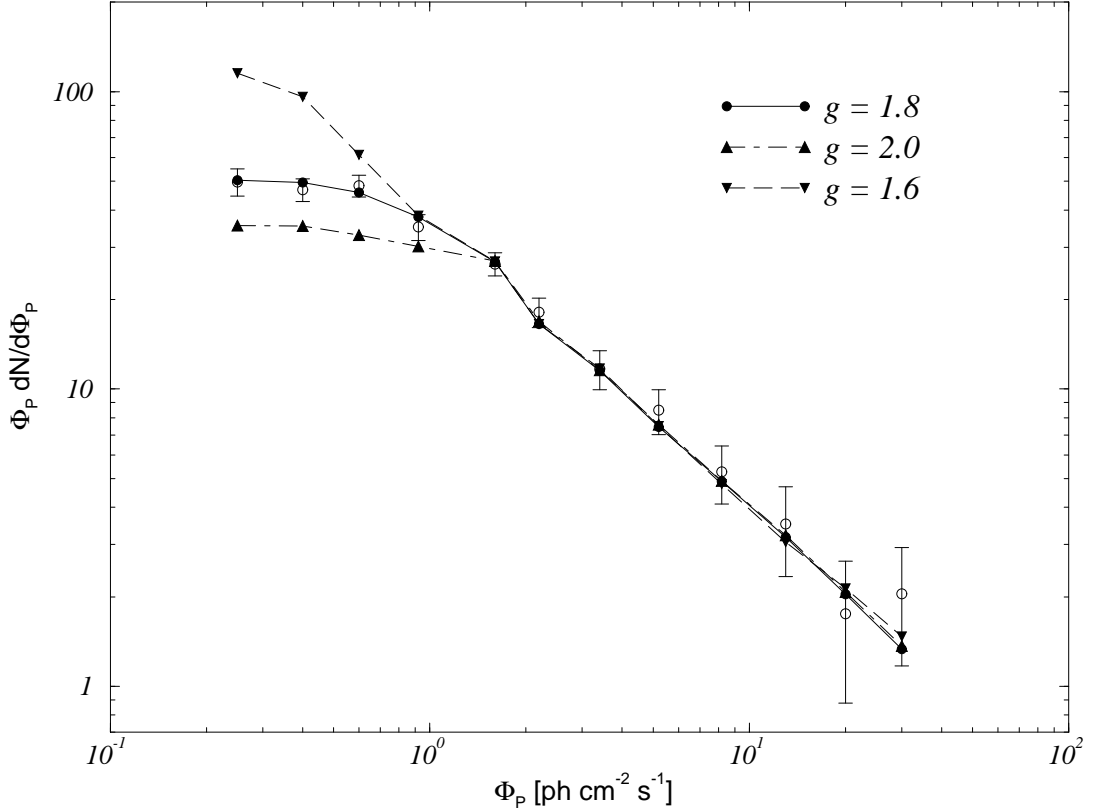


Fig. 3.— Fit of a mono-parametric GRB population (filled circles, solid line) to the 3B catalog size distribution (open circles). Burst parameters: $E_0 = 8 \cdot 10^{52}$ erg, $\Gamma_0 n_0^{1/8} = 533$ cm^{-3/8} (see text), $g = 1.8$, $q = 2.5 \cdot 10^{-4}$. Also plotted are model distributions for $g = 2$ (triangles up; dot-dashed curve) and $g = 1.6$ (triangles down, dashed curve), with all other parameters unchanged.

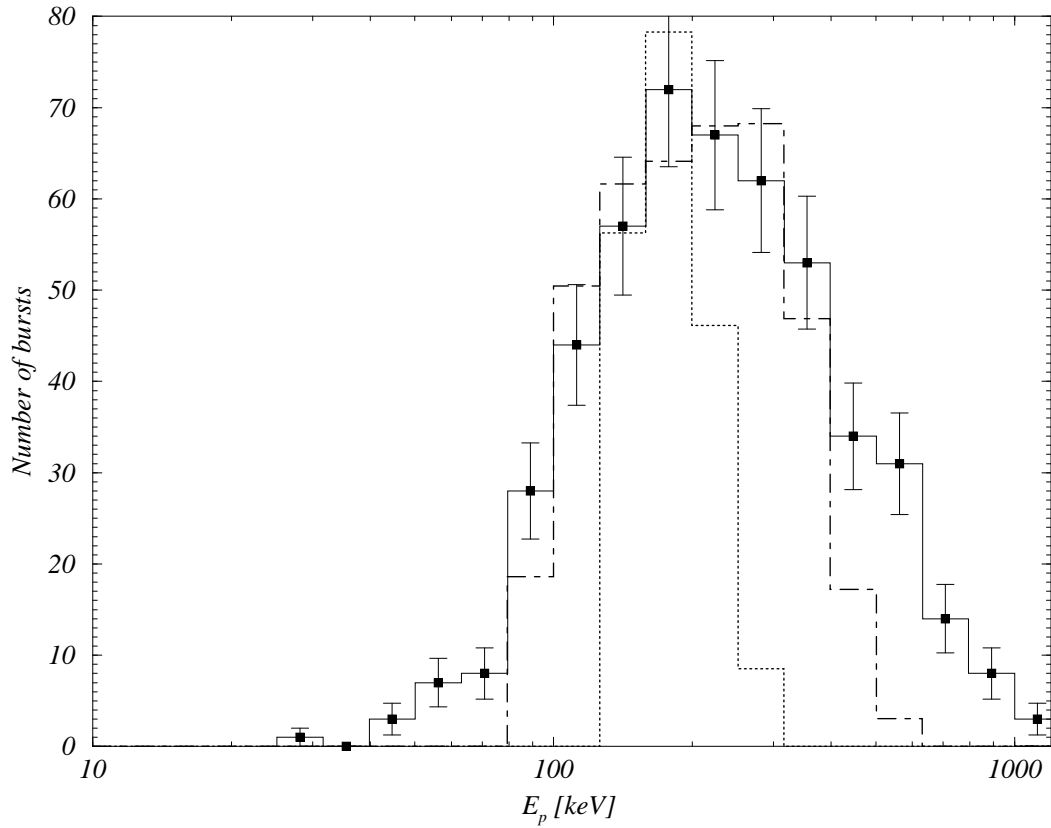


Fig. 4.— Comparison of the E_p distribution from the mono-parametric GRB population of Fig. 3 (dotted histogram) to the observed E_p distribution. The dot-dashed histogram shows the distribution resulting from a range in Γ_0 values, $115 \leq \Gamma_0 \leq 160$, and in E_0 values, $5 \cdot 10^{52} \text{ erg} \leq E_0 \leq 1.2 \cdot 10^{53} \text{ erg}$, with power-laws of index 1 in both parameters. Here we assume that $n_0 = 10^5 \text{ cm}^{-3}$, though the results remain the same if the product $\Gamma_0^8 n_0$ is constant.

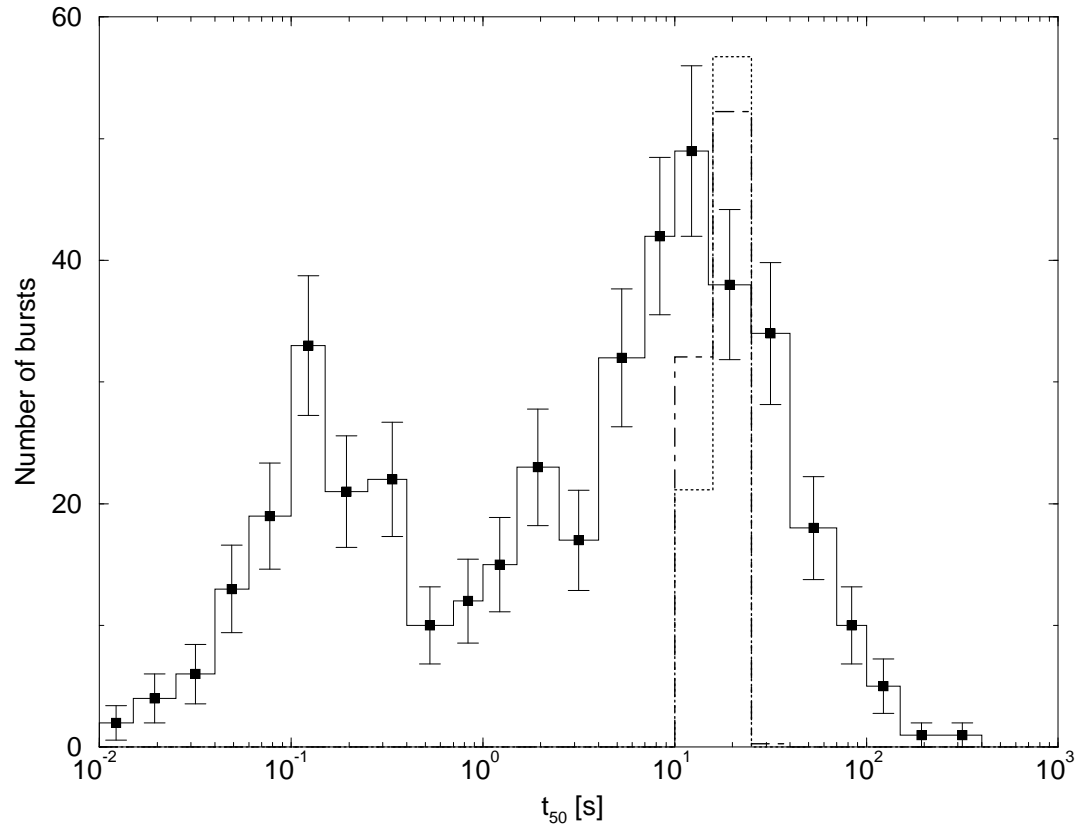


Fig. 5.— Comparison of the t_{50} distribution from the mono-parametric GRB population of Fig. 3 (dotted histogram) to the 3B catalog t_{50} distribution. The dot-dashed histogram shows the distribution from a range in Γ_0 and E_0 values — see caption of Fig. 2.

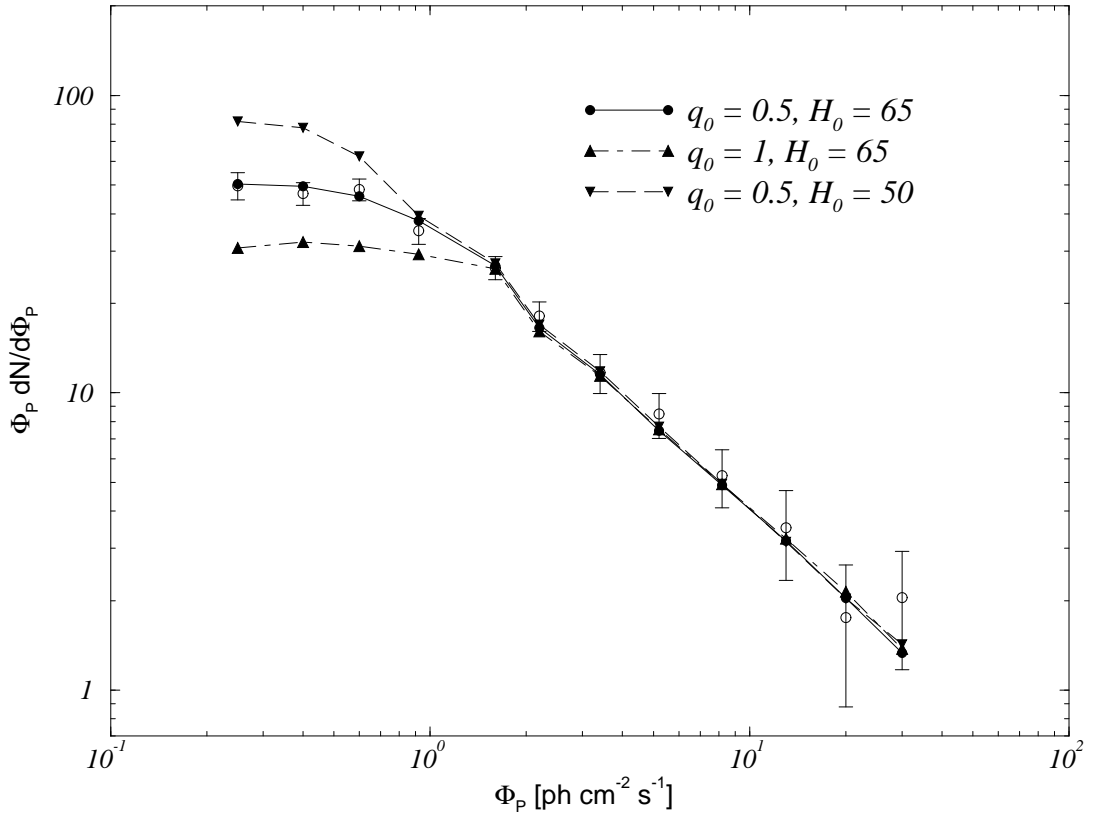


Fig. 6.— Comparison of the mono-parametric GRB population illustrated in Figs. 3 – 5 to the 3B catalog size distribution (open circles) for different cosmological parameters. The solid curve is the fit shown in Fig. 3.

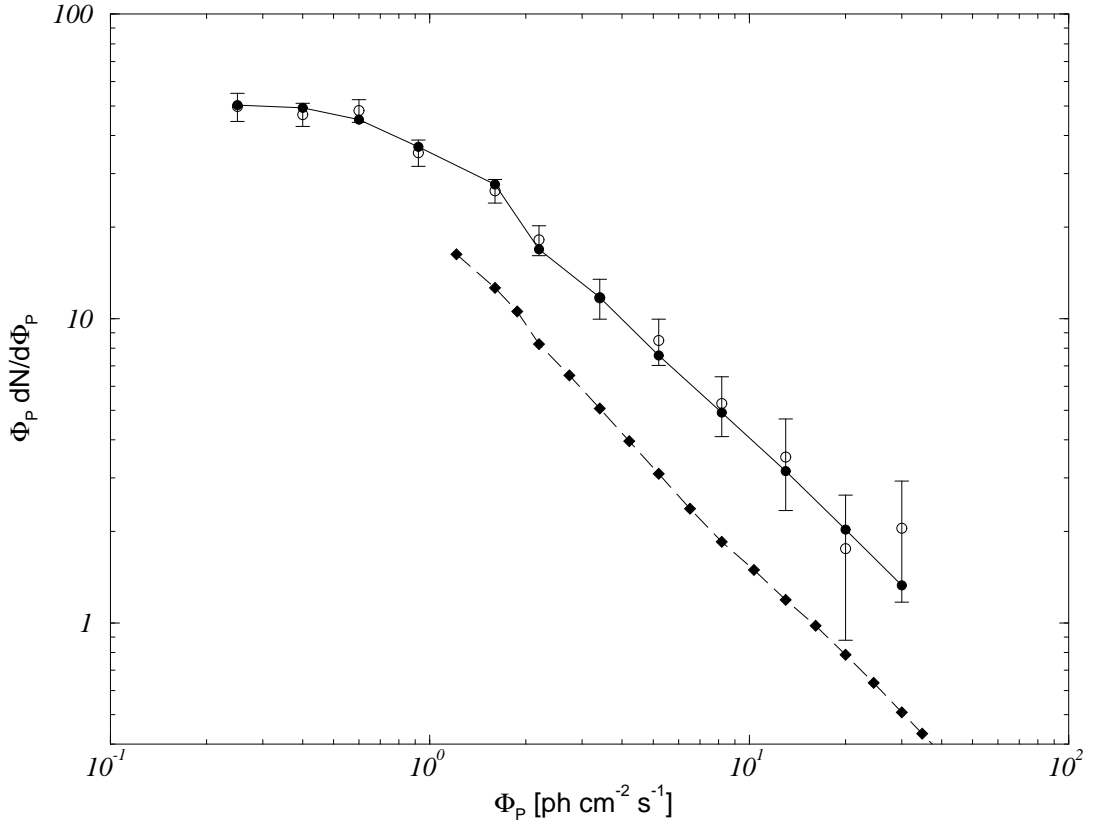


Fig. 7.— Comparison of the GRB population with $115 \leq \Gamma_0 \leq 160$ and $5 \cdot 10^{52} \text{ erg} \leq E_0 \leq 1.2 \cdot 10^{53} \text{ erg}$ (power-laws with index 1 in both parameters; solid line and filled circles) to the 3B catalog size distribution (open circles). The dashed line (filled diamonds) represents the additional sub-population of short hard bursts with $t_{50} \sim 0.1 - 0.2 \text{ s}$ and $E_p \sim 500 \text{ keV}$. Note that the data shown are extracted using only the 1024 ms trigger time scale and therefore only contain a small fraction of the short-burst population.